Hybrid FDTD Simulations of Rib–Waveguides

A. Lauer, A.Bahr and I. Wolff

Abstract—**Finite Difference Time Domain simulations of rib–waveguides on GaAs substrate are performed using a real–number hybrid (Yee/discrete–wave–equation) scheme in two dimensions. Local grid refinements are derived using equivalent circuit modifications. Discrete formulas are written using shift–operators, which make them short and easy to use. Results are compared to those obtained using the well–known effective–refractive–index (ERI) approximation. FDTD results show excellent agreement with the approximative formula, which is given in an explicit form. The refinements work well for low frequencies to determine cutoff–frequencies.**

I. Introduction

The Finite Difference Time Domain (**FDTD**) method has first been used to solve Maxwell's equations in 1966 [1]. In the recent time, growing performance of computers made it possible to use FDTD in a large scale for analysis of micro– and millimeter-wave components [2].

In this paper, rib–waveguides are analyzed using a two dimensional real–number hybrid Yee algorithm/discrete wave equation method. A similar kind of algorithm was proposed in [3] for three dimensional antenna structures.

Section II shows, how the three dimensional Yee-FDTD-scheme can be separated to generate a two dimensional real–number Yee algorithm for arbitrary lossless waveguide structures.

To save computation time and computer–memory, homogeneous regions can be simulated using a special discrete wave–equation method, which is derived from the Yee algorithm in section III.

To derive local grid refinements, section IV shows an equivalent circuit for the discrete wave–equation nodes.

In section V an approximative formula for rib–waveguides is derived with the Effective Refractive Index–Method, using a special Taylor–expansion for writing it in an explicit form.

Section VI shows a comparison of FDTD and ERI results for two sample rib–guides on GaAs–substrate.

A. Lauer, e-mail andre@ateG.uni-duisburg.de, Fachgebiet Allgemeine und Theoretische Elektrotechnik, Gerhard Mercator Universität –GH– Duisburg, D–47048 Duisburg, Germany , Phone +49 203 379 2812

I. Wolff, Fachgebiet Allgemeine und Theoretische Elektrotechnik, Gerhard Mercator Universität –GH– Duisburg, D–47048 Duisburg, Germany

A. Bahr and I. Wolff, Institute of Mobile and Satellite Communication Techniques, D–47475 Kamp-Lintfort, Germany

To the extent of the author's knowledge, the hybrid simulation method presented in this publication has not been mentioned before. It saves computation time and computer memory and gives interesting perspectives to simple local grid refinements.

II. FDTD resonator separation

For infinitely long, *lossless* waveguide structures, $\exp(j\beta z)$ dependence in the direction of propagation is considered, β given. Using this condition to separate a 3D FDTD-scheme leads to a *complex* 2D algorithm [4].

In this paper, a $\cos(\beta z)$ dependence of E_z, H_x and H_y and a $\sin(\beta z)$ dependence of H_z, E_x and E_y is assumed. This can be interpreted as putting the waveguide in a resonator with perfectly conducting planes ($z = 0$, $\beta z = \pi/2$, first resonance only) and leads to a *real* 2D algorithm.

A wave with $\exp(j\beta z)$ dependence can be generated by superposition of the resonator waves e.g. $A(\cos(\beta z) + j\cos(\beta z + 90°))$, using the translation–invariance of Maxwell's equations.

In [5] this topic is considered, too.

The 3D–Yee–FDTD scheme is

$$tH_x = H_x + \frac{\Delta_t}{\mu\Delta}\left[(1-y)E_z + (z-1)E_y\right], \quad (1)$$

$$E_x = \frac{1}{t}E_x + \frac{\Delta_t}{\epsilon_x\Delta}\left[(1-\frac{1}{y})H_z + (\frac{1}{z}-1)H_y\right], \quad (2)$$

$$\epsilon_x = \frac{1}{4}(1+\frac{1}{y}+\frac{1}{z}+\frac{1}{yz})\epsilon, \quad (3)$$

cyclic. For shortness, simpler calculations and easy implementation, shift operators and integer indices are used.

- All field components denote discrete fields, e.g. $H_x = H_x(i,j,k,n), i,j,k,n \in \mathcal{N}$, where n is the time index. $H_x(i,j,k,n)$ is at the position $(i\Delta,(j+1/2)\Delta,(k+1/2)\Delta,n\Delta_t)$, $E_x(i,j,k,n)$ is at $((i+1/2)\Delta,j\Delta,k\Delta,(n+1/2)\Delta_t)$ and so on.
- x,y,z and t are *shift operators*, e.g. $xA = A(i+1,j,k,n)$; $tA = A(i,j,k,n+1)$; $\frac{1}{t}A = A(i,j,k,n-1)$. Shift operators can be multiplied by or added to other shift operators or numbers, e.g. $xyA = A(i+1,j+1,k,n)$, $\frac{1}{xy}A = A(i-1,j-1,k,n)$ or $(5+6x)A = 5A(i,j,k,n) + 6A(i+1,j,k,n)$.
- Cyclic means from each formula *two* additional formulas can be generated by substituting ($x \to y$, $y \to z$ and $z \to x$) or ($x \to z$, $y \to x$ and $z \to y$). Shift operators as well as component indices have to be substituted.

0-7803-3246-6/96/$5.00 © IEEE

■ μ is assumed to be constant, Δ_t is the time step and Δ the step in space, assumed to be constant.

Assuming $E_z = E_z(i,j,n)\cos(\beta(k+1/2)\Delta)$ (same for H_x and H_y) and $H_z = H_z(i,j,n)\sin(\beta k\Delta)$ (same for E_x and E_y), a two dimensional FDTD-scheme for arbitrary lossless waveguides is generated :

$$tH_x = H_x + \frac{\Delta_t}{\mu\Delta}\left[(1-y)E_z + 2E_y\sin(\frac{1}{2}\beta\Delta)\right], \quad (4)$$

$$tH_y = H_y + \frac{\Delta_t}{\mu\Delta}\left[(x-1)E_z - 2E_x\sin(\frac{1}{2}\beta\Delta)\right], \quad (5)$$

$$tH_z = H_z + \frac{\Delta_t}{\mu\Delta}\left[(1-x)E_y + (y-1)E_x\right], \quad (6)$$

$$E_x = \frac{1}{t}E_x + \frac{\Delta_t}{\epsilon_x\Delta}\left[(1-\frac{1}{y})H_z + 2H_y\sin(\frac{1}{2}\beta\Delta)\right], \quad (7)$$

$$E_y = \frac{1}{t}E_y + \frac{\Delta_t}{\epsilon_y\Delta}\left[(\frac{1}{x}-1)H_z - 2H_x\sin(\frac{1}{2}\beta\Delta)\right], \quad (8)$$

$$E_z = \frac{1}{t}E_z + \frac{\Delta_t}{\epsilon_z\Delta}\left[(1-\frac{1}{x})H_y + (\frac{1}{y}-1)H_x\right], \quad (9)$$

with ϵ_x etc. obtained by substituting $\frac{1}{z}$ by 1 in the two cyclic formulas of (3), since ϵ is constant in z-direction.

Excitation is done by setting one field-component at a single point (called $F_c(P)$) to one, all others to zero as initial condition. Thus all modes with $F_c(P) \neq 0$ at β are excited. Observation of $F_c(P)$ in dependence on time and usage of the Fast–Fourier–Transform leads to sharp peaks, which denote the appropriate frequencies at β for all modes excited.

Since the usual Absorbing Boundary Conditions cannot handle the exponentially decreasing fields to be expected outside the waveguide, magnetic walls have been used as boundaries for the 2D calculations.

III. The discrete wave equation

In a homogeneous region, ϵ is constant, this means $\epsilon_x = \epsilon_y = \epsilon_z = \epsilon$. Now (4,8) and (5,7) yield

$$(T(t-1) + c^2S^2)H_x = mT(1-y)E_z + Sc^2(\frac{1}{x}-1)H_z \quad (10)$$

$$(T(t-1) + c^2S^2)H_y = mT(x-1)E_z - Sc^2(1-\frac{1}{y})H_z \quad (11)$$

with $c^2 = \frac{\Delta_t^2}{\mu\epsilon\Delta^2}$, $m = \frac{\Delta_t}{\mu\Delta}$, $T = (1-\frac{1}{t})$ and $S = 2\sin(\frac{1}{2}\beta\Delta)$.

Substituting (10,11) in (9) multiplied by $(T(t-1) + c^2S^2)$ and then divided by T gives

$$tE_z = \left[2 - \frac{1}{t} + c^2(x + \frac{1}{x} + y + \frac{1}{y} - 4 - S^2)\right]E_z, \quad (12)$$

a discrete wave equation. The same equation can be obtained for H_z.

Discontinuities are treated with the normal YEE-FDTD-scheme, (4–9).

Usage of the hybrid scheme saves approx. 33 % of computer memory and approx. 25 % of computation time.

IV. Derivation of local grid refinements

Stable local grid refinements for FDTD usage are not easy to find. Figure 1 shows the equivalent circuit for (12). Circuit analysis

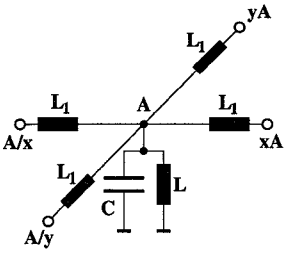

Fig. 1. Equivalent circuit for one node.

yields the time–continuous equivalent to (12),

$$\frac{\partial^2}{\partial t^2}A = \frac{1}{L_1C}(x + \frac{1}{x} + y + \frac{1}{y} - 4)A - \frac{1}{LC}A \quad , \quad (13)$$

where x,y,$1/x$,$1/y$ are shift operators and A denotes the electric potential of the node. L,L_1 and C have to be chosen appropriately, we chose $L_1 = 1$, $C = \Delta_t^2/c^2$, $L = 1/S^2$. For low frequencies,

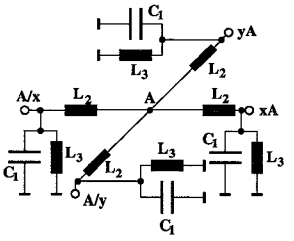

Fig. 2. Modified Equivalent circuit for one node.

the Y-Matrix of figure 1 converges against that of figure 2, with

$$L_2 = 1 + \frac{1}{4}S^2 \quad ,$$

$$L_3 = \frac{4}{S^2} + 1 \quad ,$$

$$C_1 = \frac{1}{4+S^2}\frac{\Delta_t^2}{c^2} \quad . \quad (14)$$

Now the node can be completely eliminated, re-arranging the central coils as in figure 3, with $L_4 = 4 + S^2$. No approximation is needed here fore. Thus a method to "erase" nodes is designed, e.g. allowing to erase half of the nodes in a homogeneous region as in figure 4.

Standard nodes can be erased in arbitrarily shaped homogeneous regions. To erase already modified nodes, the above procedure can be used, too.

The modified grid is stable for $\beta = 0$, because passive lumped element circuits are simulated only. For $\beta \neq 0$, instabilities were observed, but for small values of β, the results are still usable.

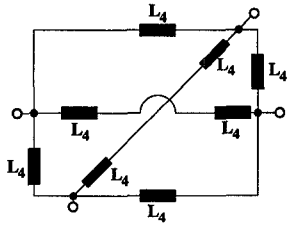

Fig. 3. Rearranged coils.

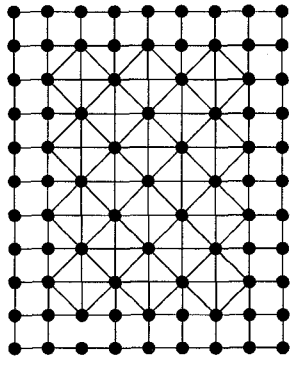

Fig. 4. Re-"fined" grid.

Erasing half of the nodes in a region reduces computer memory requirement by 50 percent. Computation time is also reduced.

V. The ERI-formula

Figure 5 shows the considered symmetric rib–waveguide on GaAs ($\epsilon_r = 12.9$).

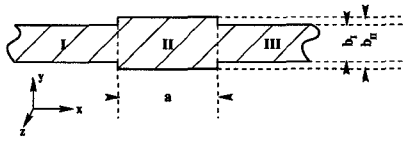

Fig. 5. Symmetric Rib–waveguide.

First ϵ_{eff} for the TE_0–film–mode (E_x,H_y and H_z only) is calculated for region (I,III) and II separately. Therefore usually

$$\tan\left(\sqrt{\epsilon_r - \epsilon_{r,\text{eff}}}\frac{\pi b}{\lambda_0}\right) = \sqrt{\frac{\epsilon_{r,\text{eff}} - 1}{\epsilon_r - \epsilon_{r,\text{eff}}}} \quad (15)$$

is solved numerically for $\epsilon_{r,\text{eff}}$ (region I) [6].

Squaring (15) and using the identity $\tan^2(\alpha) = 1/\cos^2(\alpha) - 1$ leads to

$$\cos^2\left(\sqrt{\epsilon_r - \epsilon_{r,\text{eff}}}\frac{\pi b}{\lambda_0}\right) = \frac{1}{\epsilon_r - 1}(\epsilon_r - \epsilon_{r,\text{eff}}), \quad (16)$$

$$\cos\left(\sqrt{\epsilon_r - \epsilon_{r,\text{eff}}}\frac{\pi b}{\lambda_0}\right) = \sqrt{\frac{1}{\epsilon_r - 1}}\frac{\lambda_0}{\pi b} \cdot \sqrt{\epsilon_r - \epsilon_{r,\text{eff}}}\frac{\pi b}{\lambda_0}, \quad (17)$$

$$x := \sqrt{\epsilon_r - \epsilon_{r,\text{eff}}}\frac{\pi b}{\lambda_0}, \quad (18)$$

$$k := \sqrt{\frac{1}{\epsilon_r - 1}}\frac{\lambda_0}{\pi b}, \quad (19)$$

$$\cos(x) = kx. \quad (20)$$

Using a second order Taylor expansion for $\cos(x)$, (20) can approximately be solved as

$$x \approx -k + \sqrt{k^2 + 2}. \quad (21)$$

To obtain more exact approximations, this can also be done iteratively, using the approximate x as expansion point for the next approximation. If two iterations are done, the formula gained is still explicit and usable, being exact enough for all practical cases.
This way, $\epsilon_{r,\text{eff}}$ is calculated for the regions I and II. To obtain the waveguide's effective permittivity,

$$\tan\left(\sqrt{\epsilon_{r,\text{eff,II}} - \epsilon_{r,\text{eff,wg}}}\frac{\pi a}{\lambda_0}\right) = \sqrt{\frac{\epsilon_{r,\text{eff,wg}} - \epsilon_{r,\text{eff,I}}}{\epsilon_{r,\text{eff,II}} - \epsilon_{r,\text{eff,wg}}}} \quad (22)$$

is solved the same way [6]:

$$\epsilon_i = \epsilon - \frac{\lambda_0^4}{\pi^4 b_i^4(\epsilon - 1)}\left[\sqrt{2\frac{\pi^2 b_i^2}{\lambda_0^2}(\epsilon - 1) + 1} - 1\right]^2$$

$$\epsilon_{wg} = \epsilon_{II} - \frac{\lambda_0^4}{\pi^4 a^4(\epsilon_{II} - \epsilon_I)}\left[\sqrt{2\frac{\pi^2 a^2}{\lambda_0^2}(\epsilon_{II} - \epsilon_I) + 1} - 1\right]^2$$

where the indices "r" and "eff" are left out for shortness, and i can be I or II.

VI. Results

Figure 6 shows FDTD and ERI–results for a = 300 μm, b_1 = 110 μm and b_2 = 150 μm. Δ is 5 μm, Δ_t = 7.5 fs. 65536 time–steps were used for the simulation, the simulation area is 1.5 mm x 1.5 mm (see fig. 5).
Figure 7 shows FDTD and ERI–results for a = 250 μm, b_1 = 125 μm and b_2 = 180 μm. Δ is 5 μm, Δ_t = 7.5 fs. 65536 time–steps were used for simulation, the simulation area is 1 mm x 1mm. The FDTD–simulated waveguide is *asymmetric*, its bottom is flat.
FDTD and ERI results do agree extremely well, for both, symmetric and asymmetric rib–waveguides.
The figures 8–10 show the recorded electric field of the symmetric waveguide after a Fast–Fourier–Transform has been applied to obtain the eigen–frequencies as peaks.

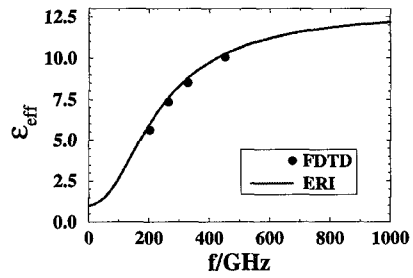

Fig. 6. FDTD and ERI–results (A).

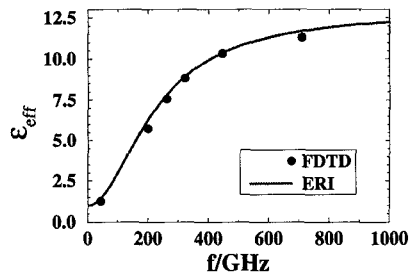

Fig. 7. FDTD and ERI–results (B).

Grid 1 is the standard Yee–grid, Grid 2 a hybrid Yee/discrete–wave–equation assembly with as many as possible nodes deleted as explained in section IV.

It can be seen, that the local grid refinements do not influence the calculated eigen–frequencies of the first few modes.

The Grid 1 simulations took approximately 2:11 hours on a MIPS–R4400 processor (200 MHz), for Grid 2 is was 1:05 hours.

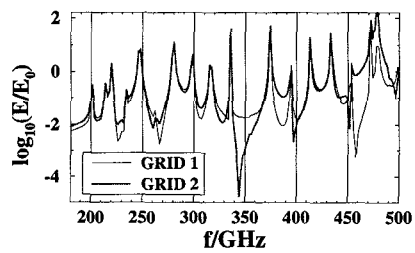

Fig. 8. Spectrum for $\beta = 10000/m$.

VII. Conclusions

The 3D Yee–FDTD scheme has been separated for a waveguide put into a resonator, so a 2D algorithm has been obtained. The results are usable for travelling wave structures, too. The 2D Yee–algorithm was then simplified in homogeneous regions, leading to a discrete wave–equation. This way, computer memory and computation time can be saved.

An explicit approximate formula was derived for rib–waveguides, its results agree very well with those of the hybrid FDTD–simulations.

Local grid refinements can be easily done in the wave–equation regions, using a special node erasing procedure. The refinements save up to 50 percent of computer memory and are accurate for low frequencies.

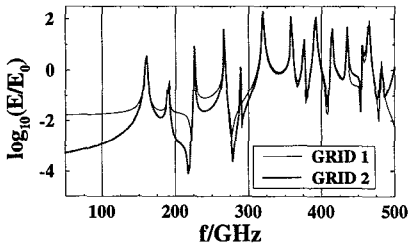

Fig. 9. Spectrum for $\beta = 0$ (TE)

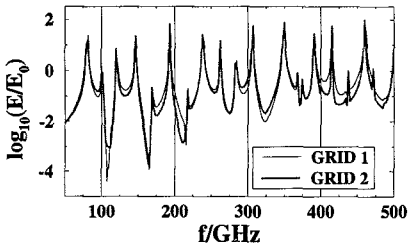

Fig 10. Spectrum for $\beta = 0$ (TM).

References

[1] Yee, K. S.: Numerical solution of initial boundary value problems involving Maxwell's equations in isotropic media *IEEE Trans. Antennas Propagation*, Vol. AP-14, pp 302-307, May 1966.

[2] Zhang, X ; Mei, K. K.: Time-domain finite difference approach to the calculation of frequency-dependent characteristics of microstrip discontinuities. *IEEE Trans. Microwave Theory Tech.*, Vol. MTT-36, pp 1775-1787, Dec. 1988

[3] Aoyagi, P H.; Lee J.; Mittra, R.: A hybrid Yee algorithm/scalar-wave equation approach, *IEEE Trans. Microwave Theory Tech.*, Vol. MTT-41, pp 1593-1600, Sep. 1993

[4] Hofschen, S.; Wolff, I.. Improvements of the 2-D-FDTD Method for the simulation of small CPWs on GaAs using time series analysis, *1994 IEEE MTT-S International Microwave Symp. Digest*, pp 39–42, San Diego, 1994.

[5] Xiao, S.; Vahldieck, R.: An efficient 2-D FDTD algorithm using real variables, *IEEE Microwave and Guided Wave Letters, Vol. 3, pp 127–129*, 1993.

[6] Adams, M.J.: An introduction to optical waveguides, Chapter 6, p 195, John Wiley & Sons, Chichester, 1981.